

## SIZE AND PURITY CONTROLLED SYNTHESIS OF SILVER NANOPARTICLES FOR MERCURY (II) ION EXTRACTION FROM AQUEOUS SOLUTIONS

AMANGELDIULY Kamar, KUZHAGALIYEVA Nursulu A., KOROBENYK Alina V.,  
WHITBY Raymond L.D.

*Nazarabayev University, Department of Chemical Engineering, Astana, Kazakhstan*

### Abstract

The formation of insoluble mercury amalgams from aqueous solution through the reaction with noble metals is a promising method for environmental clean-up. This work reports a promising avenue whereby mercury (II) ions are removed from aqueous solution using silver nanoparticles immobilized on the surface of modified silica. Commercially available fumed silica was treated with triethoxysilane in order to form silicon hydride groups on the surface. The modified silica was subsequently used in generation of silver nanoparticles on the surface of silica substrate. It was determined that the synthesized silver nanoparticles are of high purity and stably immobilized on the silica support; the concentration of silver nitrate solution and contact time between silicon hydride groups and silver ions linearly affect the size of generated metal nanoparticles. Silver nanoparticles on the silica support were tested in the process of mercury (II) ions removal.

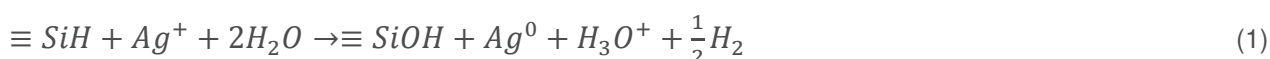
**Keywords:** Silver nanoparticles, silicon hydride groups, mercury removal, high purity, size controlled nanoparticle synthesis

### 1. INTRODUCTION

Contamination of environmental water sources by heavy toxic metals is recognized as one of the major threats faced by mankind [1, 2]. Among heavy metals, mercury is one of the most harmful pollutants, which has been paid a great attention for many decades. It is a highly toxic metal, which can accumulate and amplify in biological species along the food chain [1, 2]. Mercury exposure causes serious kidney and brain diseases [2, 3]. Therefore, development of efficient and cheap clean-up technologies for mercury removal is of great importance.

One of the rapidly developing mercury removal technologies is an adsorption which involves nanometer sized adsorbents and ion exchangers [3, 4, 5]. In comparison to bulk size particles, nanomaterials have extremely small particle size and large surface area with negligible mass transfer resistance which make separation process highly efficient [3, 4]. In the current study we propose using silver nanoparticles (Ag NPs) immobilized on silica substrate as an efficient and easily manufactured adsorbent material for mercury treatment. Silver has an ability to form an amalgam with mercury, which dissolves in the solid metal forming a solid solution. Therefore, the use of Ag NPs will allow immobilization of mercury on the surface of the silica substrate.

The chemical reduction methods have been widely used to synthesize Ag NPs from silver salts [7]. The main concern in synthesis of the metal nanoparticles by chemical reduction is attributed to instability of the particles in aqueous solutions [7, 8]. Therefore, most of the existing chemical reduction approaches make use of stabilizers in order to extend the lifetime of Ag NPs in aqueous solutions [8]. However, this results in generation of 'non-chemically pure' nanoparticles due to formation of residual groups on the surface of the adsorbent which, consequently, deteriorates adsorptive properties of the material [9]. Herein, we generate high purity Ag NPs on the surface of silica substrate by reducing silver ions from its salt solution using silicon hydride groups ( $\equiv\text{SiH}$ ). The corresponding reaction is given below in Equation (1):



Consequently, the aim of the current work is to synthesize Ag NPs of high purity and test the generated nanoparticles of different sizes in the process of mercury (II) ions removal.

## 2. EXPERIMENTAL SECTION

### 2.1. Samples Preparation

#### 2.1.1. Synthesis of surface modified silica substrate

First, the surface of fumed silica was modified via silanization reaction in which triethoxysilane (TES) reacted with fumed silica in acidic medium resulting in generation of  $\equiv\text{SiH}$  groups on the silica surface. This was realized by refluxing 3 g of fumed silica with a mixture of 0.46 ml of TES and 60 mL of glacial acetic acid for 2 hours. The final product was filtered and dried in a bench oven at 105°C for 12 hours to terminate formation of  $\equiv\text{SiH}$  groups and evaporate acetic acid and ethanol.

#### 2.1.2. Silver nanoparticles generation

At the next stage, Ag NPs were synthesized on the surface of modified silica by stirring the silica sample in  $\text{AgNO}_3$  solution. As one part of the work, the influence of silver salt concentration and contact time between  $\text{Ag}^+$  ions and  $\equiv\text{SiH}$  groups on the size of generated nanoparticles were investigated. Three nanocomposites of Ag NPs with loadings of 0.05 mmol Ag/g  $\text{SiO}_2$ , 0.1 mmol Ag/g  $\text{SiO}_2$  and 0.5 mmol Ag/g  $\text{SiO}_2$  were produced to evaluate influence of silver salt concentration. For the sake of simplicity samples were designated as SiH/Ag-x where x is the loading of silver on silica surface. The samples were synthesized from 2.5 ml, 5 ml and 25 ml of 10 mmol/l  $\text{AgNO}_3$  solution under rigorous stirring for 30 minutes. In order to investigate the effect of contact time, mixture of 5 ml of  $\text{AgNO}_3$  and 0.5 g of the hydride-modified silica was shaken for 5, 10, 15, 20 and 25 minutes. All the obtained products were filtered and dried for 12 hours at 105°C.

#### 2.1.3. Mercury adsorption experiments

Finally, mercury adsorption batch experiments were conducted with samples of SiH/Ag-0.05 and SiH/Ag-0.5 to test the efficiency of the synthesized Ag NPs on removal of mercury ions from aqueous solutions. The samples were selected on the basis of the lowest and highest silver loading. The sorption experiments were also carried out with samples of modified and fumed silica and achieved results were compared with the performance of Ag NPs. For each experiment conducted, 0.1 g of sample was impregnated into mercury acetate,  $\text{Hg}(\text{CH}_3\text{COO})_2$ , solution with pre-determined concentration. Mercury concentration in aqueous solutions was monitored in the interval from 5 to 120 minutes at room temperature and the concentration of the solutions was monitored by atomic adsorption spectrometer.

### 2.2. Samples characterization and methods of analysis

Samples were characterized using Thermo Nicolet FTIR spectrometer, Rigaku D/max 2200 Powder X-ray diffractometer (XRD) and Libra-120 Transmission Electron Microscope (TEM). Ag NPs on the silica support were tested in the process of mercury (II) ions removal. In order to verify the mercury uptake Zeeman furnace atomic-absorption spectrometer (RA-950, Lumex) was used. The amount of  $\equiv\text{SiH}$  groups grafted onto the surface of silica sample was determined using back iodometric titration technique.

## 3. RESULTS AND DISCUSSION

### 3.1. Surface modification of fumed silica

FTIR analysis showed that after the reaction of fumed silica (**Figure 1a**) with TES a sharp band appears in the spectra (**Figure 1b**) at 2260  $\text{cm}^{-1}$  identifying formation of  $\equiv\text{SiH}$  groups on the silica surface [12]. However, this

band totally disappears after the contact of modified silica with  $\text{AgNO}_3$  solution, which is a clear indication of the reduction of  $\text{Ag}^+$  ions from its salt solution and formation of Ag NPs on the modified silica substrate (**Figure 1c**). Additionally, it can be also highlighted that intensity of the stretching band, corresponding to the isolated silanol groups ( $3745\text{ cm}^{-1}$ ) on the initial silica (**Figure 1a**), have considerably decreased after the silanization reaction. Very small shoulder on the spectrum of modified silica indicates that the silanization of fumed silica has almost completely replaced silanol groups by silicon hydride groups. Other bands at 810, 1122, 1628 and  $1871\text{ cm}^{-1}$  are attributed to the internal IR standard of the fumed silica [11].

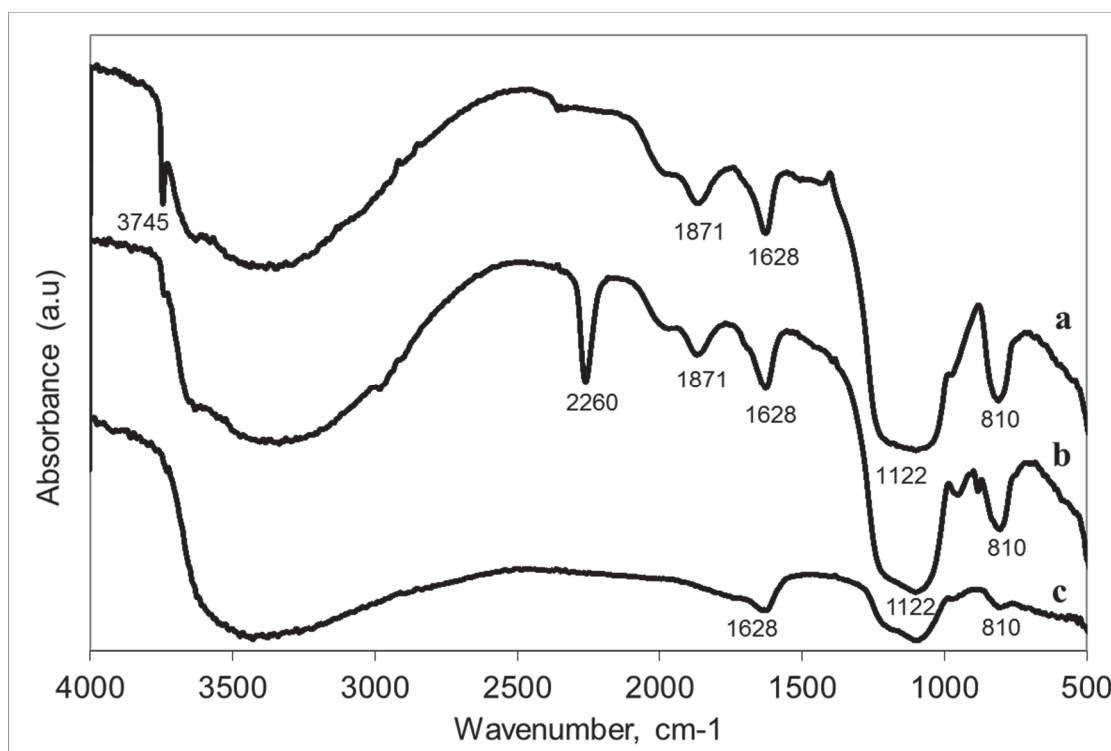


**Figure 1** FTIR spectra for fumed (a), TES modified (b) and silver nanoparticles decorated (c) silica samples

The back iodometric titration analysis showed that 0.75 mmol of  $\equiv\text{SiH}$  functional groups were synthesized per gram of  $\text{SiO}_2$ . The obtained value is in good agreement with previously reported results [10,11] and provides information on the possible amounts of silver that can be loaded onto the substrate.

## 3.2. Silver Nanoparticles generation

### 3.2.1. Effect of silver nitrate concentration

XRD analysis was performed on the nanocomposite of silica decorated with Ag NPs and X-ray diffraction patterns of Ag NPs synthesized at different concentrations of  $\text{AgNO}_3$  are given in **Figure 2**. It was found that five peaks at  $2\theta$  values of about  $38.0^\circ$ ,  $44.0^\circ$ ,  $64.0^\circ$ ,  $77.0^\circ$  and  $82.0^\circ$  corresponding to (111), (200), (220), (311) and (222) planes of silver, respectively, indicate the presence of face-centered cubic (FCC) structured crystalline Ag NPs. Validity of the obtained values was confirmed with standard powder diffraction card of silver nanoparticles (JCPDS, file No. 04-0783) [13]. A large halo at  $2\theta$  value of  $21.51^\circ$  on **Figure 2** is due to the amorphous structure of silica support. As expected no impurities in crystalline structure have been detected which indicates the high purity of the synthesized Ag NPs. The Scherrer equation was used to calculate the average sizes of the Ag NPs. Calculations yield that the average size of the crystallites for samples  $\text{Ag}/\text{SiO}_2$ -0.05 (**Figure 2a**),  $\text{Ag}/\text{SiO}_2$ -0.1 (**Figure 2b**)  $\text{Ag}/\text{SiO}_2$ -0.5 (**Figure 2c**) over highest reflection of 111 are approximately 15 nm, 20 nm and 25 nm respectively.

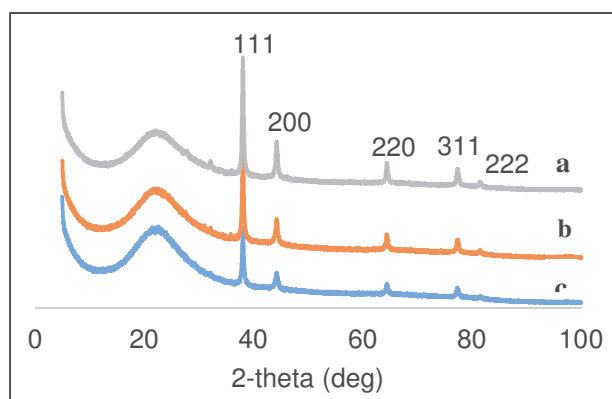


**Figure 2** X-ray diffraction patterns for Ag NPs on silica substrate synthesized from different concentration of  $\text{AgNO}_3$ : a) 0.05 mmol Ag/g  $\text{SiO}_2$ , b) 0.1 mmol Ag/g  $\text{SiO}_2$ , c) 0.5 mmol Ag/g  $\text{SiO}_2$

### 3.2.2. Effect of reaction time

TEM provided further insights into the influence of the reaction time on the size and morphology of silver nanoparticles. **Figure 3** shows that all generated nanoparticles have near-spherical shape with varying sizes.

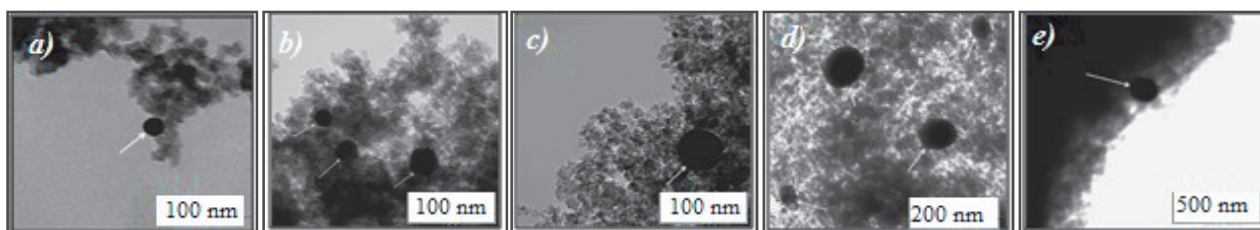


**Figure 3** TEM images of Ag NPs synthesized at different reaction times. The microscope revealed near spherical particles with sizes of a) 26 nm after 5min, b) 23 nm, 32 nm and 39 nm (from left to right) after 10 min, c) 73 nm after 15 min, d) 157 nm (left) and 78 nm (right) after 20 min, e) 171 nm after 25 min

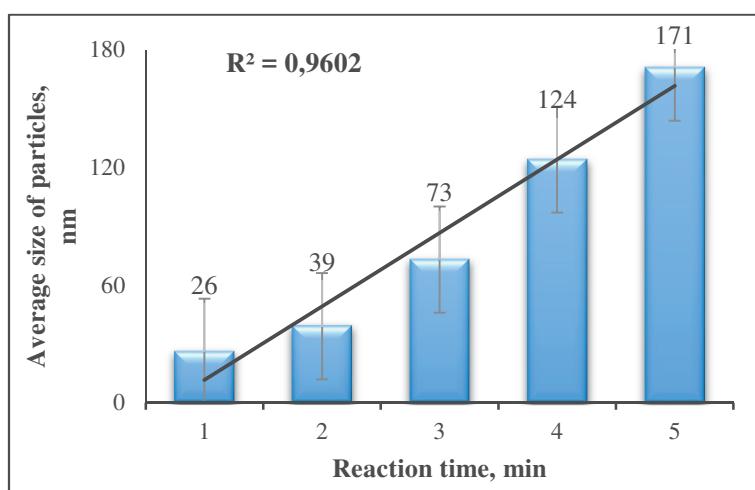


**Figure 4** Average size distribution of silver nanoparticles with respect to reaction time

It can be observed that particles are not aggregated. The surface density of the  $\equiv\text{SiH}$  groups is small and particles appear at the sites where  $\equiv\text{SiH}$  groups have been present due to highly reducing properties of the latter component which also prevents the agglomeration of the Ag NPs. Finally, stability of formed Ag NPs in aqueous solution results in increased surface area which can be favorable for mercury adsorption.

Additionally, all the synthesized nanoparticles, captured by TEM imaging system, were measured using the microscope inbuilt software to determine the influence of time contact on the size of the generated Ag NPs. Measurement results were plotted against the reaction time as shown on **Figure 4** and the percent variance of the linear trendline was calculated. It can be observed from the graph that the increase in the contact time leads to the increase in the size of the generated nanoparticles. In addition to that that the plot characterizing the size distribution of Ag NPs has almost linear character ( $R^2=0.9602$ ) with insignificant difference in particle sizes for samples obtained after 5 and 10 min of reaction. This effect can be explained by short reaction period, which was insufficient for establishment of equilibrium between silver ions and silicon hydride groups.

### 3.3. Mercury adsorption experiments

Finally, the batch experiments were conducted and the mercury uptake percentage was calculated for each sample as shown in **Figure 5**.

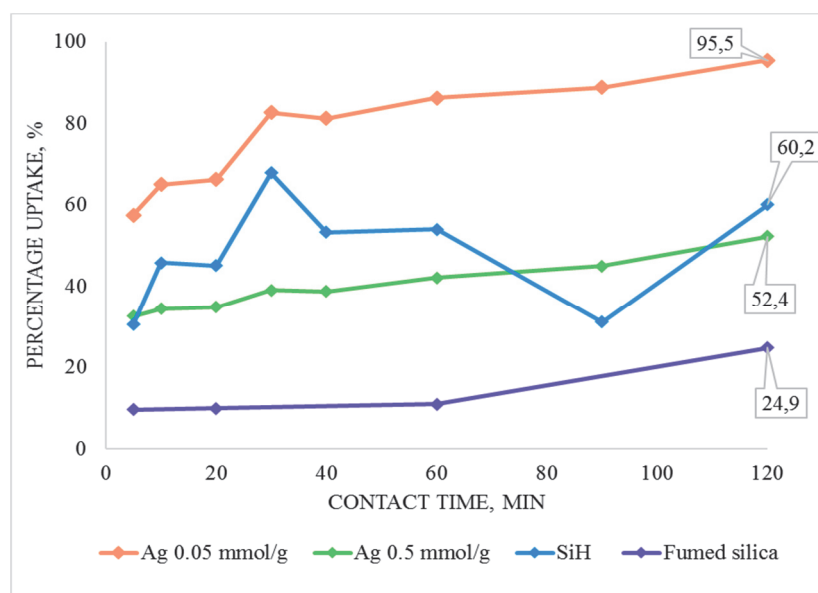


**Figure 5** Adsorption of mercury with time on different materials

It was found that amount of  $Hg^{2+}$  ions removed from solutions increased with increase in the incubation time between mercury salt solution and potential adsorbents (**Figure 5**). The results also demonstrate that both fumed and modified silica had an ability to adsorb mercury ions from  $Hg(CH_3COO)_2$  solution. However, the adsorption kinetics of mercury ions on the surface of fumed silica was found to be extremely slow and about 25% of the mercury ions was removed by this sample. The adsorption kinetics was significantly improved by modifying the surface of fumed silica with TES. The surface modification resulted in the rapid mercury removal in the first 30 minutes when about 70% of  $Hg^{2+}$  ions were extracted from mercury acetate solution. However, this figure fluctuated significantly in the remaining period of time which can be explained by the mobility of mercury on the surface of modified silica. Although silicon hydride ( $\equiv SiH$ ) groups, attached to the surface of TES modified silica, act as reducing agent towards the mercury ions, they cannot tightly “hold” mobile mercury, which tends to escape back into the solution.

However, the batch experiments shows that fluctuations in the mercury removal do not occur with samples decorated with Ag NPs that act as “anchoring” agents forming stable insoluble silver-mercury amalgams. The use of Ag NPs also considerably improved mercury uptake rate. For the sample of SiH/Ag-0.05, approximately 60% of mercury ions was extracted in just 5 minutes after commencing the experiment that could be significant enhancement in mercury adsorption processes. This figure further increased to 90% in the next hour, finally, reaching a point of 95% mercury removal at the end of the experiment ( $t=120$  min). However, the mercury

uptake decreased by almost half when another sample, SiH/Ag-0.5, with higher silver loading was tested. The decreased removal efficiency of the second sample can be attributed to the increased size of the nanoparticles, which led to decrease in their surface energy and surface area and, therefore, adsorptive qualities. The results demonstrate that nanoparticles with smaller size are more favorable for the mercury uptake.

#### 4. CONCLUSION

This study focused on removal of mercury (II) ions from aqueous solution using silver nanoparticles immobilized on the surface of modified silica substrate. It was shown that modification of fumed silica with triethoxysilane allowed to synthesize “chemically pure” silver nanoparticles whose size can also be controlled by increasing either concentration of silver nitrate solution or contact time between silicon hydride groups and silver ions. Synthesized silver nanoparticles were subsequently used in batch experiments where their effectiveness in removal of mercury ions was investigated. It was discovered that silver nanoparticles with lowest particle size had a tendency for fast and efficient mercury removal from the aqueous solution.

#### REFERENCE

- [1] BONSIGNORE, M., ANDOLFI, N., BARRA, M., MADEDDU, A., TISANO, F., INGALLINELLA, V., CASTORINA, M., SPROVIERI, M. Assessment of mercury exposure in human populations: A status report from Augusta Bay (southern Italy). *Environmental Research*, 2016, vol. 150, pp. 592-599.
- [2] ZHANG, L., WONG, M. Environmental mercury contamination in China: Sources and impacts. *Environment International*, 2007, vol. 33, no. 1, pp. 108-121.
- [3] HUBER, J., LEOPOLD, K. Nanomaterial-based strategies for enhanced mercury trace analysis in environmental and drinking waters. *TrAC Trends in Analytical Chemistry*, 2016, vol. 80, pp. 280-292.
- [4] WANG, Q., KIM, D., DIONYSIOU, D., SORIAL, G., TIMBERLAKE, D. Sources and remediation for mercury contamination in aquatic systems-a literature review. *Environmental Pollution*, 2004, vol. 131, no. 2, pp. 323-336.
- [5] EBADIAN, M. A., ALLEN, M., CAI, Y., & MCGAHAN, J. F. *Mercury contaminated material decontamination methods: investigation and assessment*. Miami: Florida International University, 2001, 61 p.
- [6] GIRGINOVA, P., DANIEL-DA-SILVA, A., LOPES, C., FIGUEIRA, P., OTERO, M., AMARAL, V., PEREIRA, E., TRINDADE, T. Silica coated magnetite particles for magnetic removal of Hg<sup>2+</sup> from water. *Journal of Colloid and Interface Science*, 2010, vol. 345, no. 2, pp. 234-240.
- [7] IRAVANI, S., KORBKANDI H., MIRMHAMMADI S.V., ZOLFAGHARI B. Synthesis of silver nanoparticles: chemical, physical and biological methods. *Research in pharmaceutical sciences*, 2014, vol. 9, no. 6, p. 385.
- [8] YERSHOV, B. G. Наночастицы металлов в водных растворах: электронные, оптические и каталитические свойства. [Metal nanoparticles in aqueous solutions: electrical, optical and catalytic properties]. *Ros. Chem. Journal*, 2001, vol. 45, no. 3, pp. 20-30.
- [9] ZHANG, F., NRIAGU, J., ITOH, H. Mercury removal from water using activated carbons derived from organic sewage sludge. *Water Research*, 2005, vol. 39, no. 2-3, pp. 389-395.
- [10] PESEK, J., MATYSKA, M. Our favorite materials: Silica hydride stationary phases. *Journal of Separation Science*, 2009, vol. 32, no. 23-24, pp. 3999-4011.
- [11] CHU, C., JONSSON, E., AUVINEN, M., PESEK, J., SANDOVAL, J. A new approach for the preparation of a hydride-modified substrate used as an intermediate in the synthesis of surface-bonded materials. *Analytical Chemistry*, 1993, vol. 65 no. 6, pp. 808-816.
- [12] KATOK, K., WHITBY, R., FUKUDA, T., MAEKAWA, T., BEZVERKHYY, I., MIKHALOVSKY, S. and CUNDY, A. Hyperstoichiometric Interaction Between Silver and Mercury at the Nanoscale. *Angewandte Chemie*, 2012, vol. 124, no. 11, pp. 2686-2689.
- [13] THEIVASANTHI, T., ALAGAR, M. Electrolytic Synthesis and Characterization of Silver Nanopowder. *Nano Biomedicine and Engineering*, 2012, vol. 4, no. 2, pp. 58-65.